Inversion of the Li–Strahler Canopy Reflectance Model for Mapping Forest Structure

Curtis E. Woodcock, *Member, IEEE*, John B. Collins, Vida D. Jakabhazy, Xiaowen Li, Scott A. Macomber, and Yecheng Wu

***Abstract*—As part of a larger forest vegetation mapping process based on Landsat TM and digitial terrain data, inversion of the Li–Strahler model provides estimates of tree size and cover for conifer stands. The vegetation maps are intended for use in natural resource management by the US Forest Service. Analysis of extensive field data in the form of "test" stands from four National Forests indicate the following about the Li-Strahler model: 1) the underlying assumptions of independence between tree size and crown shape are valid, 2) the means for tree geometry parameters vary between forest types, 3) estimates of forest cover are reliable, and 4) estimates of tree size are unreliable due to the breakdown in the relationship between image intra-stand variance and tree size. Improvements in estimates of tree size will require additional data beyond a single Landsat TM image, with multidirectional data a promising possibility.**

I. Introduction

ONE USE OF canopy reflectance models is to recover vegetation parameters from remotely sensed images, which is typically referred to as *inversion*. Many canopy reflectance models are not formulated to be invertible, and are either not invertible or difficult to invert, although considerable progress on inversion stategies is being made (see for example [1]–[7]). One explicitly invertible canopy reflectance model is the Li–Strahler model, which is formulated for use with discontinuous canopies [8]. It was originally designed for use in forests, and has been tested several times on a limited number of stands. In their original paper, Li and Strahler tested the model on two conifer stands in northern California [8]. Later, Franklin and Strahler [9] inverted the model for eight stands in a semi-arid woodland in western Africa. More recently, Franklin and Turner [10] report results from tests in the Jornada LTER in New Mexico for shrub species, and Wu and Strahler [11] used the model for the Oregon transect. In each of these papers, the Li–Strahler model is tested for each stand individually—meaning that data collected in each stand are used to parameterize and calibrate the model prior to its inversion for that stand.

This paper reports the results of tests of the Li–Strahler model in a more general context to evaluate its utility for mapping vegetation structure using Landsat TM imagery. The intent is to test how well the inversion of the model can be generalized—or parameterized and calibrated from small sets of "test" stands and then applied to many stands in an automated mapping system. This work was conducted as part of a project to map forest vegetation in the Sierra Nevada mountains of California. These vegetation maps are being produced for the U.S. Forest Service to assist with management of a variety of resources, including timber, water, and wildlife. The vegetation maps include the general vegetation classes of *hardwood* forest, *conifer* forest, *brush* and *meadow* as well as the classes *water* and *barren*. The *conifer*, *brush* and *hardwood* classes are further subdivided into species associations, or forest types, using terrain-based predicitive models [12]. For the *conifer* class two additional attributes are needed: tree size, and crown cover. The reason for using the Li–Strahler model is to provide tree size and crown cover estimates on a stand-by-stand basis for these maps. The National Forests mapped to date using the Li–Strahler model are the Tahoe, Stanislaus, Plumas, and the Lake Tahoe Basin Management Unit. An overview of the entire mapping process and general results can be found in [13]. The purpose of this paper is to present in detail the methods developed for inverting the model as part of a mapping system, and the results of tests of the model in both the Plumas National Forest and Lake Tahoe Basin.

Manuscript received July 12, 1995; revised August 23, 1996.

C. E. Woodcock, J. B. Collins, V. D. Jakabhazy, X. Li, and S. A. Macomber are with the Department of Geography and Center for Remote Sensing, Boston University, Boston, MA 02215 USA (e-mail: curtis@bu.edu).

Y. Wu is with Able Software Company, Lexington, MA 02173 USA.

Publisher Item Identifier S 0196-2892(97)02113-X.

II. Overview of the Invertible Li–Strahler Model

The Li–Strahler model is designed to estimate the size and density of trees from remotely sensed images. It is a geometric-optical model, and as such relies on the three-dimensional (3-D) structure of the canopy as the primary factor influencing reflectance from the canopy. The model assumes that the satellite measurements (pixels) are larger than the size of individual tree crowns, but still smaller than the size of forest stands. In this project, we have used an ellipsoid model for the shape of trees, with r as its half crown width, b as its vertical half-axis, and h as the height from ground to the bottom of the crown (Fig. 1). The signal received by the sensor is modeled as consisting of reflected light from tree crowns, their shadows, and the background within the field of view of the sensor. Thus, the signal can be modeled as a linear combination of four components and their areal proportions

$$S = K_g G + K_c C + K_t T + K_z Z$$

where S is the brightness value of a pixel, K_g, K_c, K_t, K_z stand for the areal proportions of sunlit background, sunlit crown, shadowed crown, and shadowed background; and G, C, T, Z are the spectral signatures of the respective components.

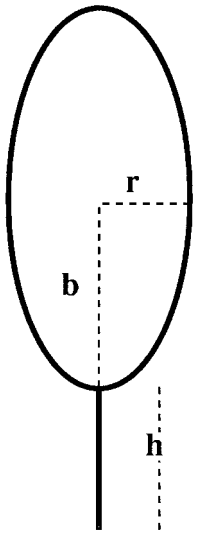

Fig. 1. This schematic drawing shows the parameters used to measure tree geometry.

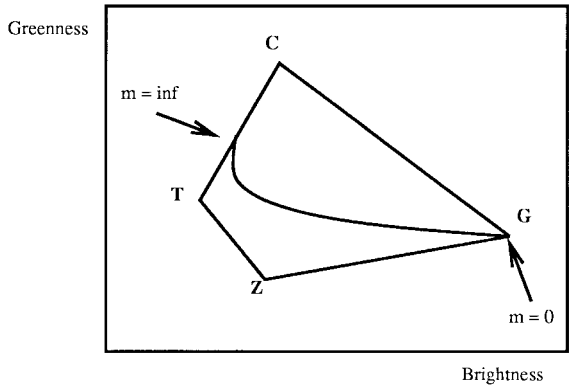

Fig. 2. This figure shows the trajectory of image values in the brightness and greenness dimensions as the number of trees is increased. C, T, G, and Z are the spectral signatures for sunlit and shadowed tree crown, and sunlit and shadowed background, respectively.

Even if we can solve for the areal proportions K_c and K_t, the problem remains of how to estimate tree crown size, because many small crowns or a few big crowns can yield the same $K_c + K_t$, or canopy coverage. The separation of effects associated with tree size and density is based on a relationship between image variance and tree size. If a homogeneous forest stand has many pixels, Li and Strahler (1985) proved that if the trees are randomly distributed (Poisson) within the stand, and crown size distribution is independent of tree density, then

$$R^2 \approx \frac{V_m}{(1+W)M}$$

where R^2 is the mean of the squared crown radius (r^2); M and V_m are the mean and variance of a "treeness" parameter m, and W is the coefficient of variation of the squared crown radius r^2. W can be easily calculated from the coefficient of variation of r, if it is lognormally distributed.

The "treeness" parameter, or m, is defined as the mean of nr^2, where n is the poisson parameter, or the number of trees per unit area. Conceptually, m is like a crown area index, and if multiplied by π would be equivalent to the proportion of the area covered by tree crowns if they did not overlap. It is an important parameter in the interface between the remote sensing signal and the forest parameters. Fig. 2 shows the spectral signatures for the scene components and how the value of S changes as m increases. When there are not any trees, $m = 0$ and the signal is simply the signature of the illuminated background (G). As trees are added and m increases, the signal moves toward a combined signature S, which is determined by the crown geometry and illumination conditions. The channels used in this graph and for the inversion of the canopy model are the standard brightness and greenness indexes from the tassled-cap transformation, calculated using the published coefficients for the Landsat TM [14].

The canopy reflectance model is based on the assumption that there are many pixels in each forest stand—the use of the variance of m (V_m) in the inversion process requires this situation. Thus, landscapes have to be partitioned into vegetation stands prior to use of the Li–Strahler model. Using Landsat TM imagery to produce maps at a scale of 1:24 000 translates into minimum sizes of vegetation stands of approximately 20 TM pixels. We use an automated image segmentation procedure to partition the TM imagery into groups of pixels, or regions, to serve as the basic map units. The image segmentation procedure is based on a multiple-pass region-growing algorithm [15].

While image segmentation is used in the automated mapping procedure, it is worth noting that the stands used in this paper were all hand-delineated on air photos. This results in better internal homogeneity within stands, and the results for this situation should be considered a best case scenario relative to image segmentation.

III. Field Data Collection and Analysis

As mentioned in the overview of the Li–Strahler model, there are several forest parameters needed for inversion of the model, including those describing the geometry of individual trees, and those pertaining to the distributional properties of trees. Additionally, there is a need to determine the spectral signatures for the four components of the model: sunlit crown and background, and shadowed crown and background. In our experience using the model, it has become clear that it is necessary to estimate these forest and image parameters separately for different forest types.

To parameterize the different forest types and calibrate the canopy reflectance model, detailed field data are collected in a number of "test" stands. The test stands are delineated on airphotos and selected to cover the range of forest types, illumination conditions, tree sizes and densities, and background conditions found in the area to be mapped. In each stand, the collection of field data is done at a series of sample sites located on a fixed grid. The intent is to distribute the sites evenly throughout the stand and remove the possibility of biasing the precise location of any individual site within the stand on the basis of the attributes of the trees in the immediate vicinity.

Data are collected at each sample site using a variable-radius plot. This approach samples trees with probability proportional to basal area, which is the horizontal area of a tree trunk at breast height. Bitterlich [16] originally developed the method, and it has become commonly used in forest sampling [17]. It is referred to as a "variable-radius" plot because there is a different size area sampled for each size of tree. Larger trees can be farther from the sighting point and still be sampled. An angle gauge is used to determine whether each tree should be tallied. An exact solution based on an equation using the distance from the sighting point and the diameter at breast height (DBH) of the tree is used for trees too close to judge using optical instruments. The angle gauges are calibrated to a specific basal area factor (BAF), meaning that any tree counted at a sample point represents the same contribution to the estimate of the basal area per unit area. For example, using a 10 m^2/hectare BAF prism, if six trees are tallied at a site, then the estimate of basal area is 60 m^2 per hectare. For each tree included at a site, the species and DBH are recorded. Additional measurements at each site are made for a single *measure tree*, including the height, crown width and height-to-crown.

A. Tree Geometry Parameters

One underlying assumption of the model is that the ratios describing tree shape are independent of tree size. This assumption means, for example, that the overall shape of an ellipsoid as measured by the ratio of the major to the minor axis (b/r) does not change as trees become larger. Similarly, the proportion of the height of the entire tree covered by tree crown is assumed constant and independent of tree size. The data from the measure trees in the tests stands allow evaluation of these assumptions for the first time. Fig. 3(a)–(c) shows the values for each of the three tree geometry ratios, r/b, $b + h/r$ and h/b (see Fig. 1), plotted as a function of DBH, which is a common measure of tree size. These scatter plots do not indicate any trends in the data, and are the first data presented to support the assumptions of the model. As a further precaution, the data in these graphs were sorted by forest types and species and plotted separately. To save space, these graphs are not presented here, but they also do not exhibit any trends between the various ratios and tree size.

The different forest types often do have different mean values for the tree geometry ratios, indicating that different conifer species tend to have different shapes. The means for the three tree geometry ratios for each forest type are given in Table I. This table shows that trees in the red fir zone have relatively narrow crowns, while trees in the eastside pine have wider crowns that extend further down the trunk of the tree.

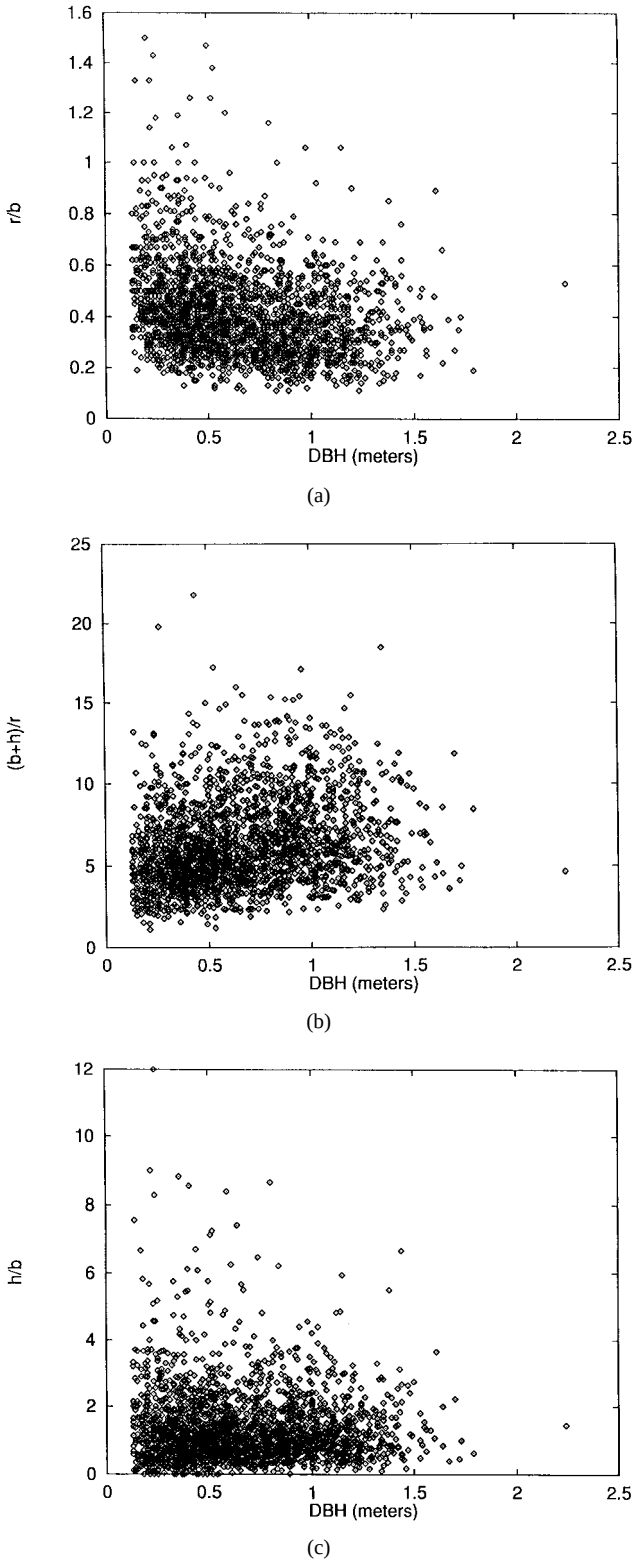

Fig. 3. (a)–(c) These figures show the relationship between various ratios of tree shape parameters and tree size. The lack of relationship illustrated in these graphs is an underlying assumption of the Li–Strahler model.

B. Estimating Parameters for the Test Stands

To calibrate the model there is a need to know the mean tree size, density, and the mean and variance of m for each test stand. All of these can be calculated from the field data. The mean stand density (n), defined as the number of trees per pixel (900 m^2 in this case) is calculated from the test stand data as follows

$$n = k \sum_{i=1}^{N_x} \sum_{j=1}^{N_{y_i}} \frac{B}{0.000\,078\,45 D_{ij}^2}$$

TABLE I
VALUES OF THE VARIOUS TREE GEOMETRY RATIOS FOR DIFFERENT FOREST TYPES. SEE FIG. 1 FOR THE MEANING OF THE GEOMETRY RATIOS

Forest Type	b/r	b/h	b+h/r
Eastside Mixed Conifer	2.64	1.23	6.06
Eastside Pine	2.39	1.75	4.87
Mixed Conifer	2.77	1.24	6.01
Red Fir	3.49	1.30	7.65
Westside Pine	2.81	0.99	6.66

TABLE II
RESULTS OF REGRESSIONS OF CROWN DIAMETER ON DBH FOR VARIOUS FOREST TYPES

Forest Type	intercept	slope	R^2
Eastside Mixed Conifer	2.837	0.304	0.720
Eastside Pine	3.487	0.314	0.556
Mixed Conifer	4.602	0.246	0.506
Red Fir	4.292	0.181	0.462
Westside Pine	4.202	0.277	0.559

where there are N_x points per stand and N_y trees per point; D is DBH of tree j in point i, measured in centimeters; B is the basal area factor (in the units of m^2 per hectare), and k is the number of hectares per pixel. For each stand, D can be calculated as follows

$$D = \frac{k}{n}\left[\sum_{i=1}^{N_x}\sum_{j=1}^{N_{y_i}} D_{ij}\frac{B}{0.000\,078\,45D_{ij}^2}\right].$$

A more useful measure of tree size when using the Li–Strahler model is mean crown radius, R. To convert D to R, a simple linear regression based on the data from the measure trees is used. Table II shows the regression results for five major forest types. Notice that crown width increases more slowly as a function of DBH for trees in the red fir forest type than for the others.

From the estimates of crown diameter (R) and density (n) it is possible to calculate the mean of the m-values (or M) as

$$M = nR^2.$$

Similarly, the variance (V_m) can be calculated as

$$V_m = R^2M(1+W)$$

where W is the coefficient of variation of the size distribution, which is calculated as the ratio of the mean to the variance of the square of the crown radii measurements.

IV. ESTIMATION OF COMPONENT SIGNATURES

As described earlier, the model has four component spectral signatures, G, C, T and Z representing the sunlit background, sunlit crown, shadowed crown and shadowed background, respectively. The component signatures are used throughout the canopy model inversion process, and their estimation has been one of the primary issues involved in attempting to use the Li–Strahler model for forest mapping over large areas.

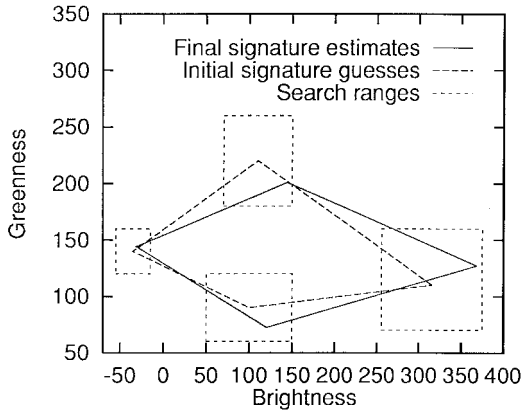

Fig. 4. This graph illustrates the search range (boxes) for signatures around initial guesses (dashed line), and the final estimates of the component signatures (solid line). The example given is the red fir forest type in the Plumas National Forest.

The method used for signature estimation relies heavily on the data from the test stands. The heart of the signature estimation is the comparison of m-values as calculated from the field data with m-values estimated by the model using a certain set of component signatures. The "best" set of components signatures is defined as the one that minimizes the total difference between the field measured and model estimated mean of m. The search for the "best" set of component signatues begins with a hand-selected set based on a graph of the brightness and greenness values from the test stands. Then, random sets of signatures are drawn from within a user-specified range in brightness and greenness values for each of the component signatures (Fig. 4). Each set of signatures is used to estimate m-values for each of the test stands, and the signatures eventually used are the "best" fit.

The signatures selected using this approach are shown in Fig. 4 for the red fir forest type in the Plumas National Forest. These signatures are similar to the ones selected manually, but the component signatures for sunlit tree crown and background are "brighter." Fig. 5 shows the estimated component signatures for five forest types in the Plumas National Forest. These results exhibit several interesting patterns. As expected there is little variation in T, the shadowed tree crown. Also as expected, there is considerable variation in G, the background signature. Third, there is a surprising amount of variation in the estimates for Z, the shadowed background. The unusually bright estimates for Z appear to be caused by under estimates of m by the model for some of the test stands. A bright value for Z increases the model estimates for m.

Alternative methods exist for the calibration of the component signatures. One possibility would use ground-based spectral measurements of the various components [18]. This approach was impractical for this application for several reasons. First, there were several forest types for which component signatures were required. It would have been logistically impossible to collect component signatures for the different regional forest types at the same time as the satellite overpass. Second, we did not always know which date of satellite imagery we would be using at the time the field data were collected. Since this approach would require atmospheric

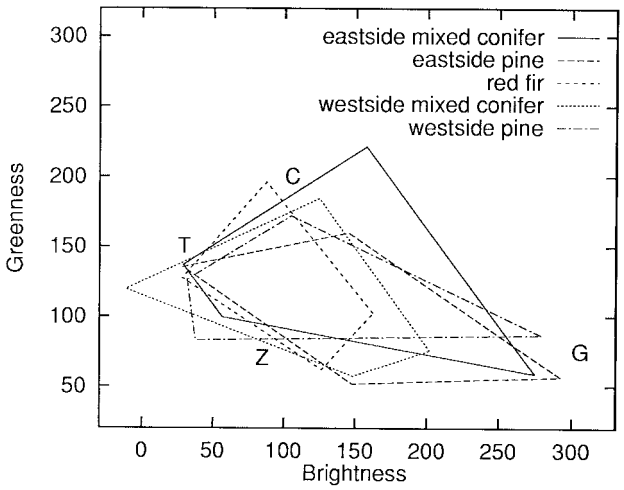

Fig. 5. This graph shows all final component signatures for the various forest types in the Plumas National Forest. Of interest is the fact that some components vary more between forest types than others.

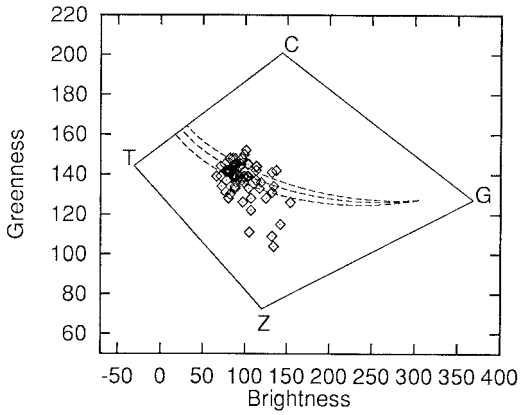

Fig. 6. This graph illustrates the behavior of the 2-D look-up-table used to estimate the value of m for each pixel. The different lines represent different values for the b/r ratio.

correction of the satellite imagery to use the ground-based spectral measurements, it would have been necessary to make measurements of atmospheric conditions at the time of the satellite overpass.

One issue related to the estimation of component signatures concerns their stability and the amount of field data required. Since a field crew of two people can typically collect the necessary data for only one test stand per day, these data are expensive. In our mapping projects, where there may be four or five different forest types within a National Forest, we have typically used eight test stands per forest type. The data from the Tahoe Basin, where there are 26 test stands within a single forest type allow exploration of the stability of the estimates of component signatures. For this test, the signatures were estimated first using all the test stands, and then twice separately using half, and then finally four times using a quarter of the test stands. As the true signatures are unknown, the difference between the signatures estimated from the entire dataset serves as a measure of stability. Signatures that vary dramatically for a subset of data would be considered unstable. Comparison of results for these different amounts of data indicate little change in the stability between the datasets with half and a quarter of the tests stands. This indicates that there may be small incremental improvement associated with the addition of more test stands.

A. Two-Dimensional Look-Up-Table

If tree crowns all have the same shape, then all pixels will fall along a line from G (zero crown cover) to a point between C and T (full coverage, or X_∞) (see Fig. 2). However, practical situations are never so ideal—pixels usually form a scatter around the line. If the scatter is narrow around the line, it is unimportant, but if the scatter is wide it can adversely affect the estimation of both the mean and variance of m. The scatter is caused partly because of variation in the background signature G, and partly because of variation in the crown shape. For relatively sparse forest stands, the variation in the background signature is dominant; while for dense forest stands, the shape of crowns is dominant [8]. Li and Strahler [8] employed a two-dimensional (2-D) look-up-table to reveal the variation in m values caused by changing crown apex angles for their earlier version of the model that used cones as the shape of trees. A similar technique and argument can be applied for ellipsoidal trees by using the variation in the ratio of the crown width/height (r/b) in place of the apex angle. For this approach, a two-dimensional look-up table is used for the estimation of *m-values* for each pixel in a stand.

The creation of a 2-D look-up-table uses "forward modeling," meaning that we assume all unknowns of a pixel are known, and solve for the resulting location in the brightness/greenness plane. Then a table is constructed for every combination of m and b/r ratios for a given set of component signatures. Then this table is used to find the m value and b/r ratio for each pixel in a stand. Fig. 6 illustrates graphically the nature of a 2-D look-up table. In this figure, each line from G to X_∞ corresponds to a different b/r ratio. For estimating an *m-value*, each pixel is projected to the closest of the three lines. This approach improves the estimate of m for brightness and greenness pairs that are not close to the original line between G and X_∞.

B. Topography

One level of correction for topography is directly incorporated in the Li–Strahler model; the way in which the proportions of the components (K_g, K_c, K_t, K_z) change as a function of the cosine of the local solar zenith angle $(\cos\Theta_o)$ is solved on a stand-by-stand basis. This corrects for the lengthening of shadows on slopes facing away from the sun and the foreshortening of shadows on slopes facing the sun. However, tests on images illustrated that not only do the proportions of the components change, but the signatures also change. Thus, we have adopted an additional correction for topography based on adjustment of the brightness of the signature for G based on the reasoning below.

It has long been observed that topographic effects are minimal in greenness images so their correction for topography is unnecessary. Correction of the brightness image for the cosine of the local solar zenith angle compensates for the change

in beam illumination on the different topographic surfaces [19]. Using this kind of correction, the brightness of all pixels in the image could be changed instead of changing the signatures. However, careful examination of the model reveals that all the component signatures should not be corrected. The intensity of illumination on tree crowns (components C and T) should not be influenced by the local solar zenith angle, since trees are aligned by gravity rather than normal to the slope. The intensity of the illumination on the background on a slope, on the other hand, is proportional to the cosine of the local solar zenith angle. Thus, we correct the brightness signal of the illuminated background, G, by the cosine of the illumination angle on a stand-by-stand basis using digital terrain data. Graphically (Fig. 4), this correction is the shifting of G horizontally. We have not bothered to correct Z, the shadowed background, as it is assumed to be stable and primarily affected by diffuse effects.

V. Results

While the outputs from the model are tree size and density, to understand the behavior of the model it is most helpful to evaluate first the estimates of the mean and variance of m. Fig. 7(a) and (b) shows the relationship between field measurements and model estimates of m for the mixed conifer and eastside pine forest types in the Lake Tahoe Basin. Fig. 8(a) and (b) shows the results for the variance of m for the same test stands as Fig. 7. From these results it is clear that the mean of m is being estimated much more effectively than the variance of m. Table III shows R^2 values for simple linear regressions between field measured and model estimated values for the mean and variance of m, tree crown radius (R), stand density (n), and crown cover (c). Crown cover is one of the desired output features in our vegetation maps, and can be calculated as a function of crown radius and count density as follows

$$c = 1 - e^{-n\pi r^2}.$$

The results in Table III include both the Plumas National Forest and the Lake Tahoe Basin. Both sets of results indicate that the mean of m is being estimated more effectively than the variance of m. Since the estimates of crown radius are directly dependent on the variance of m, the crown radius results mirror those for the variance of m. Fig. 9 shows the expected relationship between crown radius and the variance of m for a range of values for the mean of m. Fig. 10 shows the observed pattern in this relationship, where lines connect test stands with similar means for m. These figures illustrate the heart of the problem for tree size estimation, which is the mismatch between observed and expected patterns between tree size and image variance.

When interpreting the results for density in Table III, it is useful to remember that tree size is estimated in the model prior to tree density. If the estimate of the mean of m is correct and the estimate of crown radius is wrong, it is impossible for the estimate of density to be correct. Cover, on the other hand, is closely related to the mean of m, and thus is more accurately estimated.

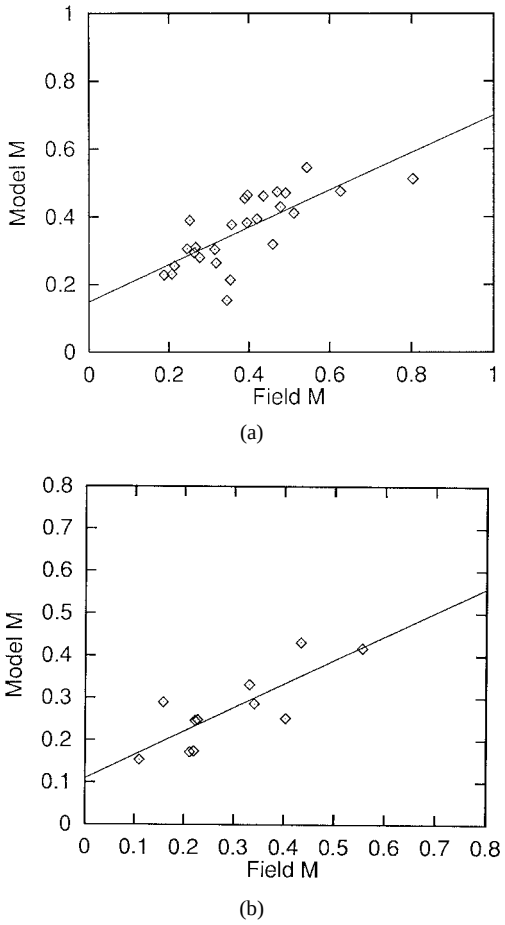

Fig. 7. These graphs show the relationships between field-measured values model estimates for m for test stands in the Lake Tahoe Basin for the (a) mixed conifer and (b) eastside pine forest types, respectively.

With respect to topography, the ideal results would be independence between error in the estimation of m and the cosine of the local solar zenith angle $(\cos\Theta_o)$. Fig. 11 shows the difference between m-values as estimated by the model and measured in the field for the test stands in the Lake Tahoe Basin plotted as a function of $\cos\Theta_o$. Each test stand appears twice—once when the same signature for G_b is used for all stands, and once when G_b is corrected by $\cos\Theta_o$ for each stand. The uncorrected data show a stronger slope with respect to $\cos\Theta_o$, indicating the correction by $\cos\Theta_o$ helps. However, the slope for the $\cos\Theta_o$ corrected results is not zero, indicating the correction does not entirely solve the problem.

VI. Discussion

One clear message from the results presented above is that the Li–Strahler model can not be used to estimate tree size in an automated mapping system based on single date Landsat TM imagery. This relationship is also indicated by two kinds of prior results presented by Woodcock *et al.* [13]. First, patterns in the field-measured timber volumes for strata based on estimates from the Li–Strahler model for tree size and cover show consistent increases in timber volume for increasing cover, but not for increasing tree size. Second, thematic map accuracies for cover classes are higher than for tree size

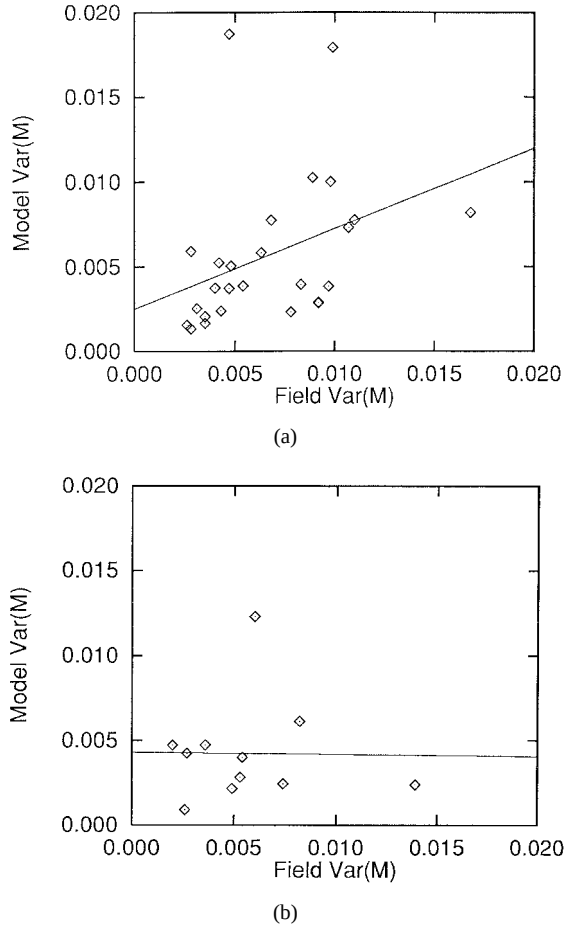

Fig. 8. These graphs show the relationships between field-measured values model estimates for the variance of m for test stands in the Lake Tahoe Basin for the (a) mixed conifer and (b) eastside pine forest types, respectively. This poor relationship is the basis of the tree size estimation problems.

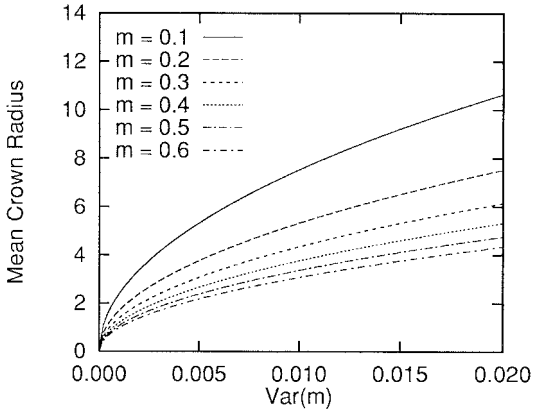

Fig. 9. This graph illustrates the expected relationship between crown radius (R^2) and the variance of m for a range of values for the mean of m.

classes. The results presented in this paper clearly identify that the problems arise from a poor relationship between field measurements of tree size and the observed variance of m estimated from images.

To understand the meaning of these results and their causes it is instructive to review the underlying theory. The spatial variance in images is a complex function of the number and

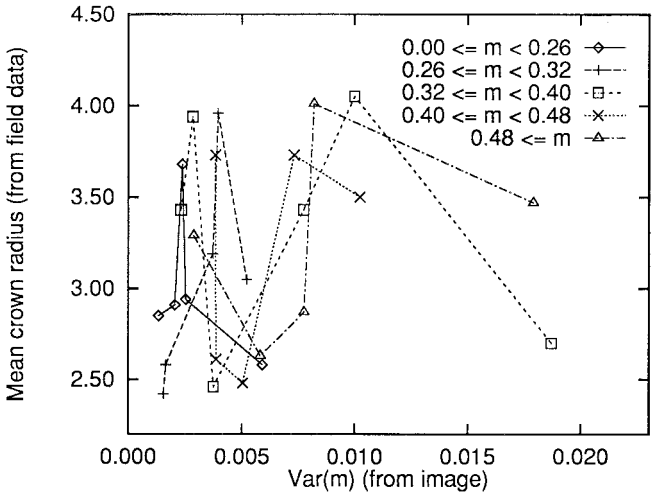

Fig. 10. This graph shows the observed relationship between crown radius (R^2) and the variance of m for a range of values for the mean of m.

TABLE III
RESULTS OF THE MODEL INVERSION FOR TEST STANDS FROM FOUR NATIONAL FORESTS. THE RESULTS ARE SHOWN IN THE FORM OF LINEAR REGRESSION RESULTS BETWEEN MODEL ESTIMATES AND FIELD MEASUREMENTS. IN THE SECOND COLUMN β_o IS THE INTERCEPT AND β_1 IS THE SLOPE. R^2 IS A MEASURE OF THE STRENGTH OF ASSOCIATION. THE COLUMN HEADED BY "m" REFERS TO THE m VALUE OF THE MODEL, AS EXPLAINED IN THE TEXT. 'VAR(M)' REFERS TO THE VARIANCE OF m VALUES

		m	var(m)	crown radius	count density	cover	number of stands
Plumas							
Eastside	β_0	0.03	-0.00	4.60	14.03	-0.00	7
Pine	β_1	0.71	1.15	-0.68	0.35	0.86	
	R^2	0.61	0.22	0.10	0.59	0.65	
Eastside	β_0	0.07	-0.00	2.86	25.23	0.17	8
Mixed	β_1	0.58	2.69	0.10	0.02	0.59	
Conifer	R^2	0.46	0.17	0.00	0.00	0.26	
Red	β_0	0.03	0.00	2.89	-22.87	0.05	8
Fir	β_1	0.94	0.63	0.15	1.77	0.93	
	R^2	0.93	0.24	0.00	0.55	0.93	
Westside	β_0	0.21	0.01	-2.65	-21.83	0.32	9
Mixed	β_1	0.24	-0.68	2.04	1.56	0.41	
Conifer	R^2	0.16	0.05	0.07	0.62	0.15	
WP	β_0	0.07	-0.01	-13.31	25.76	0.13	6
	β_1	0.71	7.26	6.60	-0.31	0.76	
	R^2	0.89	0.52	0.37	0.09	0.89	
Tahoe Basin							
Eastside	β_0	0.11	0.00	3.99	27.87	0.23	11
Pine	β_1	0.56	-0.01	-0.34	0.30	0.58	
	R^2	0.65	0.00	0.11	0.05	0.60	
Mixed	β_0	0.15	0.00	0.89	26.92	0.22	26
Conifer	β_1	0.55	0.47	0.61	0.67	0.65	
	R^2	0.55	0.13	0.12	0.20	0.49	

the size of trees and the spatial resolution of the remote sensor, and it is the separation of these effects that is difficult. Li and Strahler [8] provide the mathematics underlying their model, but a more physical understanding of the process involved is helpful here. For this approach, there is relevant theory based on a simplified model for scenes of discs randomly distributed on a contrasting background, where the binomial distribution can be used. The analogy to a forest scene is simple, with discs serving as trees. The main difference from the Li–Strahler model is the removal of effects related to shadows. Following the notation of Jupp *et al.* [20], the proportion of an area left

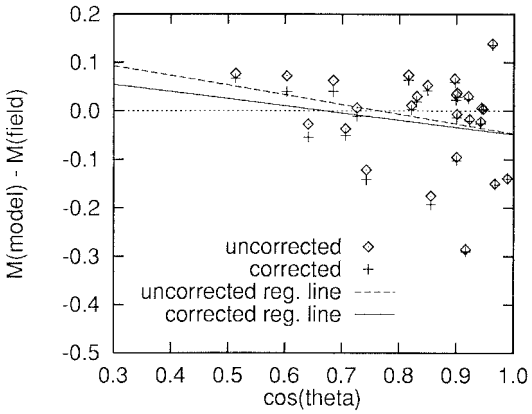

Fig. 11. This graph illustrates the effect of the topographic correction based on adjustment of the component signature of the sunlit background (G) by the cosine of the local solar zenith angle. The reduction in the slope of the regression line following correction indicates that topographic effects have been reduced. The fact that the slope is not zero indicates topographic effects have not been removed.

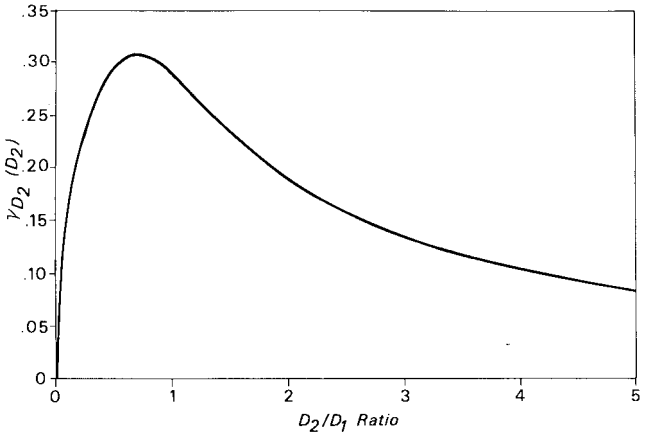

Fig. 12. This figure was originally printed in [25], and shows the relationship between local variance and the ratio between scene object sizes and the spatial resolution of remotely sensed measurements. D_2 is the spatial resolution, and D_1 is the object size, with γ_{D_2} measuring the value of the variogram at a lag of one pixel. For the present case, it illustrates the reason within-stand variance should increase with tree size, as the spatial resolution of the sensor is several times larger than the trees.

uncovered (Q_1) by λ discs of area A is

$$Q_1 = e^{-\lambda A}.$$

The binomial variance is simply $Q_1(1-Q_1)$, which approaches zero at both low and high values of Q_1, and peaks in the middle of the distribution. This simple relationship illustrates that variance is directly related to cover, which is the combined effect of both object size and count density. This relationship describes the fundamental underlying properties of a simple binomial scene, but ignores the effects associated with observation of the scene via remote sensing. In particular, it does not take into account the effects of pixel size, or regularization, on the measurements made from such a scene. Fig. 12, which is from Jupp *et al.* [21], graphically illustrates the combined effects of pixel size and object (or disc) sizes on spatial variance. In this figure, D_2 corresponds to the diameter of pixels, and D_1 to the diameter of discs (or trees in our case), and constant values for disc size and count density are used to generate this graph. The y-axis is the value of the variogram at a lag of one pixel, hence the term "local variance." Starting at values near zero for D_2/D_1, the pixels are smaller than objects, and the local spatial variance is low due to the likelihood that neighboring pixels fall on the same object, or gap between objects. For large values of D_2/D_1, (i.e., greater than 4 or 5), spatial variance is again low as there are many objects in each pixel, and the proportions of Q_1 within pixels becomes more stable. This situation is analagous to the remote sensing of trees using 30 m Landsat TM data, and has previously been called the L-resolution case [22]. Note that as the D_2/D_1 ratio decreases toward unity that spatial variance continues to increase. In our case, since pixel size is fixed, increasing tree size decreases the D_2/D_1 ratio, and should result in an increase in spatial variance. These ideas form the basis of the relationship exploited in the Li–Strahler model—which were not found to hold for the test stands in the conifer forests of the Sierra Nevada mountains. The question that remains is why the observed data do not match the theory.

There are several possibilities. First, and probably most important, is that the relationship between image variance and tree size is dependent on the assumption that once cover related effects are removed, tree size is the only factor influencing intra-stand variance. Or, at the very least, tree size is the dominant factor controlling image variance. One condition required for this assumption is that all the scene components are constant in reflectance, so that the relative mix of components determines variance, not the within component variance. While it is unreasonable to expect no variance within the scene components, it is at least required that the within-component variance is small in magnitude relative to the variance introduced by differences in tree size. While this assumption may be reasonable for trees, it is probably unreasonable for the background. In the Sierra Nevada mountains, a wide range of background materials, and hence reflectance are encountered. This situation is common even within the same stand. Backgrounds vary from exposed rock, to soil and leaf litter, to a sparse herbacious understory, to a dense understory of shrubs or hardwood trees.

In this respect, the Li–Strahler model behaves much like a spectral mixture model and is thus subject to the weaknesses of such models. Variance in end members in a spectral mixture model will degrade results in the same way that variance in the component signatures will here. In essence, the significant difference between the Li–Strahler model and other mixture models is that the combinations of components that can occur is limited. Related to the question of signatures of components is the issue of multiple scattering. When used for forward modeling, or estimation of the reflectance from a forest stand of known attributes, the Li–Strahler model has been criticized for not directly considering multiple scattering within the canopy. For inversion purposes, the component signatures represent a combined signature including the effects of beam and diffuse irradiance and all orders of scattering. The signatures are estimated empirically, so there is no need to try to quantify the individual effects.

Another factor that influences variance estimates from images is the spatial distribution pattern of trees. Any spatial patterns diverging from random, or the poisson distribution, will adversely affect variance estimates. Disturbance due to selective cutting of trees tends to produce more clumped distributions, which increase measured values of the variance of m in images. In the model, these inflated estimates of m result in over estimation of tree size. This effect was noted in many areas. In essence, any factor that increases variance unrelated to tree size will undermine the inversion results.

The finding that cover can be estimated from the Li–Strahler model is not surprising. A number of authors have empirically demonstrated the relationship between cover and various spectral bands and vegetation indicies [23], [24]. The question that remains to be answered concerns the benefits associated with using the Li–Strahler model to estimate cover as compared with simpler regression-based methods. To answer this question, a more direct comparison with regression-based methods is needed. The Li-Strahler model explicitly incorporates the effects of topography and thus should preform better than regression-based methods, but the magnitude of the benefits are unclear at this time.

The major research question that remains concerns future methods for estimating tree size. One possible line of research would be to improve the use of spatial statistics in the inversion process. Chen *et al.* [25] have developed a method for separating the effects of disc size and density using zero-hit run-length statistics derived from images. However, their results indicate that the method is only effective for the H-resolution case, or when trees are either larger than pixels or of similiar size. Jupp [26] has developed an inversion strategy based on variograms, but its utility for forest mapping remains untested. The advantage of Jupp's method is that it incorporates local spatial variance, or spatial variance at lags prior to the sill, directly in the inversion process. Viewed from this perspective, the Li-Strahler model only uses the sill of the variogram. Similarly, St-Onge and Cavayas [27] have pursued methods of empirically estimating tree size from the range of variograms. Their results with simulated images are encouraging, but further tests on real images are needed. It also appears their methods will be limited to high resolution images, i.e., when pixels are smaller than individual trees.

Other opportunities for improved size estimation could come from improvements in the remote sensing data. For example, multiple look angles such as provided by ASAS would provide additional data that should help improve inversion results. Even multitemporal imagery, if the images have different solar geometry should prove helpful, as image variance would change between images as a function of solar zenith angle.

VII. Conclusion

Tests of the inversion of the Li–Strahler model in support of efforts to develop automated procedures for mapping forest structure have found the following: 1) the tree geometry assumptions underlying the Li–Strahler model hold in the conifer forests of Sierra Nevada mountains; 2) the means for tree geometry parameters differ across forest types; 3) the Li–Strahler model can be used in automated mapping of forest cover, but tree size estimation is unreliable; 4) the cause of the problems in tree size estimation is the unreliable relationship between image intra-stand variance and tree size; 5) the topographic correction procedure used helps but does not entirely solve the problem; 6) component signatures estimated from test stands are relatively stable, meaning that there is little change associated with increased numbers of test stands.

Acknowledgment

The authors would like to thank Region 5 of the USDA Forest Service, R. Warbington and J. Levitan for help in many phases of this research, S. Ryherd and N. Shaw for field data collection, and J. Harward for programming. A. Strahler provided extensive help and encouragement throughout. We also thank three anonymous reviewers for helpful comments and suggestions.

References

[1] N. S. Goel and R. L. Thompson, "Inversion of vegetation canopy reflectance models for estimating agronomic variables–IV: Total inversion of the sail model," *Remote Sens. Environ.*, vol. 15, pp. 237–253, 1984a.

[2] ———, "Inversion of vegetation canopy reflectance models for estimating agronomic variables. V. Estimation of leaf area index and average leaf angle using measured canopy reflectances," *Remote Sens. Environ.*, vol. 16, pp. 69–85, 1984b.

[3] N. S. Goel, "Models of vegetation canopy reflectance and their use in estimation of biophysical parameters from reflectance data," *Remote Sens. Rev.*, vol. 4, pp. 1–212, 1988.

[4] J. Otterman, "Inferring parameters for canopies nonuniform in azimuth by model inversion," *Remote Sens. Environ.*, vol. 33, pp. 41–53, 1990.

[5] B. Pinty, M. M. Verstrate, and R. E. Dickinson, "A physical model of the directional reflectance of vegetation canopies. 2. Inversion and validation," *J. Geophys. Res.*, vol. 95, no. D8, pp. 11767–11775, 1990.

[6] A. Kuusk, "Determination of vegetation canopy parameters from optical measurements," *Remote Sens. Environ.*, vol. 37, pp. 207–218, 1991.

[7] F. Baret, S. Jacquemoud, B. Andrieu, M. Danson, and K. Jaggard, "Model inversion to retrieve canopy characteristics from high spectral resolution data," in *Proc. Sixth Int. Symp. Physic. Measur. Spectral Signatures*, Val d'Isere, France, Jan. 17–21, 1994, pp. 181–192.

[8] X. Li and A. H. Strahler, "Geometric-optical modeling of a conifer forest canopy," *IEEE Trans. Geosci. Remote Sens.*, vol. GRS23, pp. 705–721, Sept. 1985.

[9] J. Franklin and A. H. Strahler, "Invertible canopy reflectance modeling of vegetation structure in semiarid woodland," *IEEE Trans. Geosci. Remote Sens.*, vol. 26, pp. 809–825, 1988.

[10] J. Franklin and D. L. Turner, "The application of a geometric optical canopy reflectance model to semiarid shrub vegetation," *IEEE Trans. Geosci. Remote Sens.*, vol. 30, pp. 293–301, Mar. 1992.

[11] Y. Wu and A. H. Strahler, "Remote estimation of crown size, stand density, and foliage biomass on the Oregon transect," *Ecolog.. Applicat.*, vol. 4, pp. 299–312, 1993.P

[12] S. Macomber, C. E. Woodcock, R. Warbington, and K. Casey, "Modeling species associations for vegetation maps using terrain rules," *GRASS'91 Users Conf.*, Berkeley, CA, 1991, pp. 137–148.

[13] C. E. Woodcock, J. B. Collins, S. Gopal, V. D. Jakabhazy, X. Li, S. Macomber, S. Ryherd, Y. Wu, V. J. Harward, J. Levitan, and R. Warbington, "Mapping forest vegetation using landsat TM imagery and a canopy reflectance model," *Remote Sens. Environ.*, vol. 50, pp. 240–254, 1994.

[14] E. P. Crist and R. C. Ciccone, "A physically-based transformation of thematic mapper data—The TM tasseled cap," *IEEE Trans. Geosci. Remote Sens.*, pp. 809–825, 1984.

[15] C. E. Woodcock and J. Harward, "Nested-hierarchical scene models and image segmentation," *Int. J. Remote Sens.*, vol. 13, no. 16, pp. 3167–3187, 1992.

[16] L. R. Grosenbaugh, "Point sampling and line sampling: Probability theory, geometric implications, synthesis," *USFS So. For. Exp. Sta. Occ.*, New Orleans, LA, paper no. 160.

[17] J. R. Dilworth and J. F. Bell, *Variable Probability Sampling*, Oregon State University Book Stores Inc., Corvallis, p. 130, 1978.
[18] Schaaf, C. Barker, X. Li, and A. H. Strahler, "Validation of bidirectional and hemispherical reflectances from a geometric-optical model using ASAS imagery and pyranometer measurements of a spruce forest," *Remote Sens. Environ.*, vol. 49, pp. 138–144, 1994.
[19] J. Dozier and A. H. Strahler, "Ground investigations in support of remote sensing," *Manual of Remote Sens.*, R. N. Colwell, Ed., 2nd Edition, Amer. Soc. Photogrammetry, vol. I, 1983, pp. 959–986.
[20] D. L. B. Jupp, A. H. Strahler, and C. E. Woodcock, "Autocorrelation and regularization in digital images I: Basic theory," *IEEE Trans. Geosci. Remote Sens.*, vol. 26, pp. 463–473, July 1988.
[21] ———, "Autocorrelation and regularization in digital images II, simple image models," *IEEE Trans. Geosci. Remote Sens.*, vol. 27, pp. 247–258, May 1989.
[22] A. H. Strahler, C. E. Woodcock, and J. A. Smith, "On the nature of models in remote sensing," *Remote Sens. Environ.*, no. 20, pp. 121–139, 1986.
[23] J. Franklin, "Thematic mapper analysis of coniferous forest structure and composition," *Int. J. Remote Sens.*, vol. 7, no. 10, pp. 1287–1301, 1986.
[24] D. L. Peterson, W. E. Westman, N. J. Stephenson, V. G. Ambrosia, J. A. Brass, and M. A. Spanner, "Analysis of forest structure using thematic mapper simulator data," *IEEE Trans. Geosci. Remote Sens.*, vol. GRS24, pp. 113–121, Nov. 1986.
[25] R. Chen, C. E. Woodcock, A. H. Strahler, and D. L. B. Jupp, "Nonlinear estimation of scene parameters from digital images using zero-hit run-length statistics," *IEEE Trans. Geosci. Remote Sens.*, vol. 31, no. 3, pp. 735–746, 1993.
[26] D. L. B. Jupp, *Inversion of the Disk Images Using Mean, Variance and Variogram Data*, in preparation, 1997.
[27] B. A. St.-Onge and F. Cavayas, "Estimating forest stand structure from high resolution imagery using the directional variogram," *Int. J. Remote Sens.*, vol. 16, no. 11, pp. 1999–2021, 1995.

Curtis E. Woodcock (M'90) received the B.A., M.A., and Ph.D. degrees from the Department of Geography, University of California, Santa Barbara.

Since 1984 he has taught at Boston University, where he is currently Associate Professor and Chair of Geography and a Researcher in the Center for Remote Sensing. His primary research interests in remote sensing include mapping and inventory of forests and other natural environments, spatial modeling of images and inversion of reflectance models, and image processing and geographic information systems. He is also interested in the detection of environmental change using remote sensing.

Dr. Woodcock is a member of the American Society of Photogrammetry and Remote Sensing.

John B. Collins, photograph and biography not available at the time of publication.

Vida D. Jakabhazy, photograph and biography not available at the time of publication.

Xiaowen Li, photograph and biography not available at the time of publication.

Scott A. Macomber, photograph and biography not available at the time of publication.

Yecheng Wu received the B.A. degree in computer science from Beijing University of Aeronautics and Astronautics, the M.A. degree in image processing and remote sensing from Chinese Academy of Science, and the Ph.D. degree from the Department of Geography, Boston University.

Since 1990, he has worked at developing computer software systems, such as auomated DNA sequencing, gel electrophoresis image analysis, 3-D microscopy imaging system, industrial ultrasonic inspection system, and automated raster to vector conversion system. In 1994, he founded Able Software Co., Lexington, MA, to develop automated raster to vector conversion system for GIS and CAD applications and is currently the President. His primary research interests include automated raster to vector conversion and image pattern recognition, 3-D image reconstruction; medical image processing, spatial modeling of images and inversion of reflectance models, and geographic information systems. He is also interested in computer software engineering issues, including object oriented design and programming, algorithm optimization and artificial intelligence.